Open

Oncogene (2013) **32,** 1135–1143

www.nature.com/onc

ORIGINAL ARTICLE

The NF2 tumor suppressor regulates microtubule-based vesicle trafficking via a novel Rac, MLK and p38^{SAPK} pathway

RF Hennigan[1], CA Moon[1], LM Parysek[2], KR Monk[3], G Morfini[4,5], S Berth[4,5], S Brady[4,5,6] and N Ratner[1,5,6]

Neurofibromatosis type 2 patients develop schwannomas, meningiomas and ependymomas resulting from mutations in the tumor suppressor gene, *NF2*, encoding a membrane-cytoskeleton adapter protein called merlin. Merlin regulates contact inhibition of growth and controls the availability of growth factor receptors at the cell surface. We tested if microtubule-based vesicular trafficking might be a mechanism by which merlin acts. We found that schwannoma cells, containing merlin mutations and constitutive activation of the Rho/Rac family of GTPases, had decreased intracellular vesicular trafficking relative to normal human Schwann cells. In *Nf2* $-/-$ mouse Schwann (SC4) cells, re-expression of merlin as well as inhibition of Rac or its effector kinases, MLK and p38^{SAPK}, each increased the velocity of Rab6 positive exocytic vesicles. Conversely, an activated Rac mutant decreased Rab6 vesicle velocity. Vesicle motility assays in isolated squid axoplasm further demonstrated that both mutant merlin and active Rac specifically reduce anterograde microtubule-based transport of vesicles dependent upon the activity of p38^{SAPK} kinase. Taken together, our data suggest loss of merlin results in the Rac-dependent decrease of anterograde trafficking of exocytic vesicles, representing a possible mechanism controlling the concentration of growth factor receptors at the cell surface.

Oncogene (2013) **32,** 1135–1143; doi:10.1038/onc.2012.135; published online 23 April 2012

Keywords: merlin; NF2; Rac; trafficking; exocytosis

INTRODUCTION

Neurofibromatosis type 2 is an inherited autosomal dominant disease characterized by bilateral schwannomas of the 8th cranial nerve.[1–3] The tumor suppressor gene responsible for this disorder, *NF2,* is also inactivated in spontaneously arising tumors, including schwannoma, meningioma and malignant mesothelioma, thus implicating it in a range of human cancers.[4] Targeted deletion of *Nf2* in Schwann cells leads to schwannoma formation in the mouse.[5] The *NF2* gene encodes merlin, a 70-kDa member of the ezrin, radixin, moesin (ERM) family of membrane-cytoskeleton adapter proteins. The precise mechanisms by which merlin functions as a tumor suppressor are poorly understood.

Merlin shares a conserved secondary structure with other members of the ERM family consisting of an N-terminal FERM domain, followed by a central α-helical region and a C-tail domain.[6] Transition between the open, FERM-accessible conformation and the closed, FERM-inaccessible conformation controls merlin tumor suppressor function and is modulated by phosphorylation of serine 518.[7] Phosphorylation of S518 correlates with a growth-permissive state and is a key point of integration of merlin activity with signal transduction pathways.[8,9] Under growth-suppressive conditions, merlin is activated upon dephosphorylation of S518 by cellular phosphatases such as MYPT1-PP1δ.[10] Inactivation of merlin is achieved by the action of the small GTPase, Rac, via its effector kinase, PAK, resulting in phosphorylation of merlin at S518.[11,12] Merlin in turn antagonizes Rac activity by an unknown mechanism, forming a negative feedback loop of mutual inhibition.[13] This antagonism appears to be lost in human schwannomas because these merlin-deficient cells are characterized by constitutive activation of Rac.[14–16] *Nf2*-null cells grow to abnormally high densities *in vitro*, and it has been suggested that this loss of contact inhibition is the biological basis for schwannoma formation.[17,18] Merlin is thought to control contact inhibition by regulating the cell surface availability of growth factor receptors.[19,20] However, the mechanisms by which merlin, and perhaps activated Rac, affects growth factor receptor abundance are unclear.

We found that merlin-deficient tumor cells show decreased intracellular vesicular trafficking relative to normal human Schwann cells. Significantly, this effect was dependent upon the activity of Rac and the MAP kinase p38^{SAPK}. Inhibition of Rac and the effector kinase MLK3 also impaired growth in merlin null cells at high density. In *Nf2* $-/-$ SC4 Schwann cells, re-expression of merlin or inhibition of Rac, MLK or p38^{SAPK} all resulted in increased velocity of exocytic vesicles. In a squid axoplasm system, open conformation mutants of merlin and active Rac each specifically reduced fast anterograde axonal vesicle transport. This effect was independent of the plasma membrane and dependent upon the activity of p38^{SAPK}. Together these data show that the loss of merlin reduces microtubule-based exocytic vesicle velocity in a Rac-MLK-p38^{SAPK}-dependent manner. We propose that merlin-Rac signaling may normally modulate vesicle release from microtubules, influencing concentrations of growth factor receptors at the cell surface.

[1]Division of Experimental Hematology and Cancer Biology, Cincinnati Children's Hospital Medical Center, Cincinnati, OH, USA; [2]Department of Cell and Cancer Biology, University of Cincinnati School of Medicine, Cincinnati, OH, USA; [3]Department Genetics, Washington University School of Medicine, St Louis, MO, USA; [4]Department Anatomy and Cell Biology, University of Illinois at Chicago, Chicago, IL, USA and [5]Marine Biological Laboratory, Woods Hole, MA, USA. Correspondence: Dr RF Hennigan, Division of Experimental Hematology and Cancer Biology, Cincinnati Children's Hospital Medical Center, 240 Albert Sabin Way, Cincinnati, OH 45229, USA.
E-mail: Robert.Hennigan@cchmc.org
[6]These authors contributed equally to this work.
Received 20 January 2012; revised 7 March 2012; accepted 9 March 2012; published online 23 April 2012

RESULTS

VAMP-2 vesicle mobility is reduced in schwannoma cells in a Rac- and p38^{SAPK}-dependent manner

To determine if loss of merlin expression affects intracellular vesicular trafficking, we designed an assay to measure the mobility of a subset of membrane-bounded organelles in live primary normal human Schwann cells relative to live, patient-derived primary human schwannoma cells. To visualize internal vesicle motion by time-lapse imaging, we marked transfected cells with a plasmid expressing GFP fused to the ubiquitously expressed v-SNARE protein, VAMP2/synaptobrevin 2.[21–24] The relative mobility of VAMP2-GFP-positive vesicles was used as a measure of general intracellular trafficking (Figure 1). Primary cultures were transfected with plasmids expressing a VAMP2-GFP fusion protein and general mobility was quantified by measuring the percentage of VAMP2-GFP-positive vesicles that changed position between successive 3 s intervals over 180 s. Normal human Schwann cells showed highly motile VAMP2-positive vesicles with a broad range of values, (Figure 1c) with a mean and s.e.m. of 4.2 ± 0.1%. In contrast, primary human schwannoma cells had a more restricted range of values (Figure 1d), with a mean and s.e.m. of 2.0 ± 0.1%, suggesting an inhibition of intracellular membrane traffic in tumor relative to normal cells. As loss of merlin expression results in activation of Rac,[13] we measured VAMP-2 in schwannoma cells treated with the specific Rac inhibitor NSC23766.[25] Rac inhibition significantly increased VAMP-2 mobility (Figure 1e), mean and s.e.m. of 6.0 ± 0.1%. The MAP kinase, p38^{SAPK} functions downstream of Rac and has been shown to phosphorylate and inhibit kinesin heavy chain, thereby implicating it in the regulation of trafficking.[26] Treatment of schwannoma cells with the p38^{SAPK} inhibitor, SB203580, significantly increased VAMP-2 mobility (Figure 1f), mean and s.e.m. of 5.8 ± 0.1%. These data implicated a Rac-p38^{SAPK} pathway as regulating intracellular trafficking in schwannoma cells.

Rac regulates high density growth in merlin null cells

The results of the VAMP2 experiments suggested that Rac controls a p38^{SAPK}-dependent pathway that regulates intracellular vesicle motility. We next tested if this pathway was required to mediate the major biological consequence of merlin mutation, loss of contact inhibition of growth.[27] *Nf2−/−* merlin-deficient

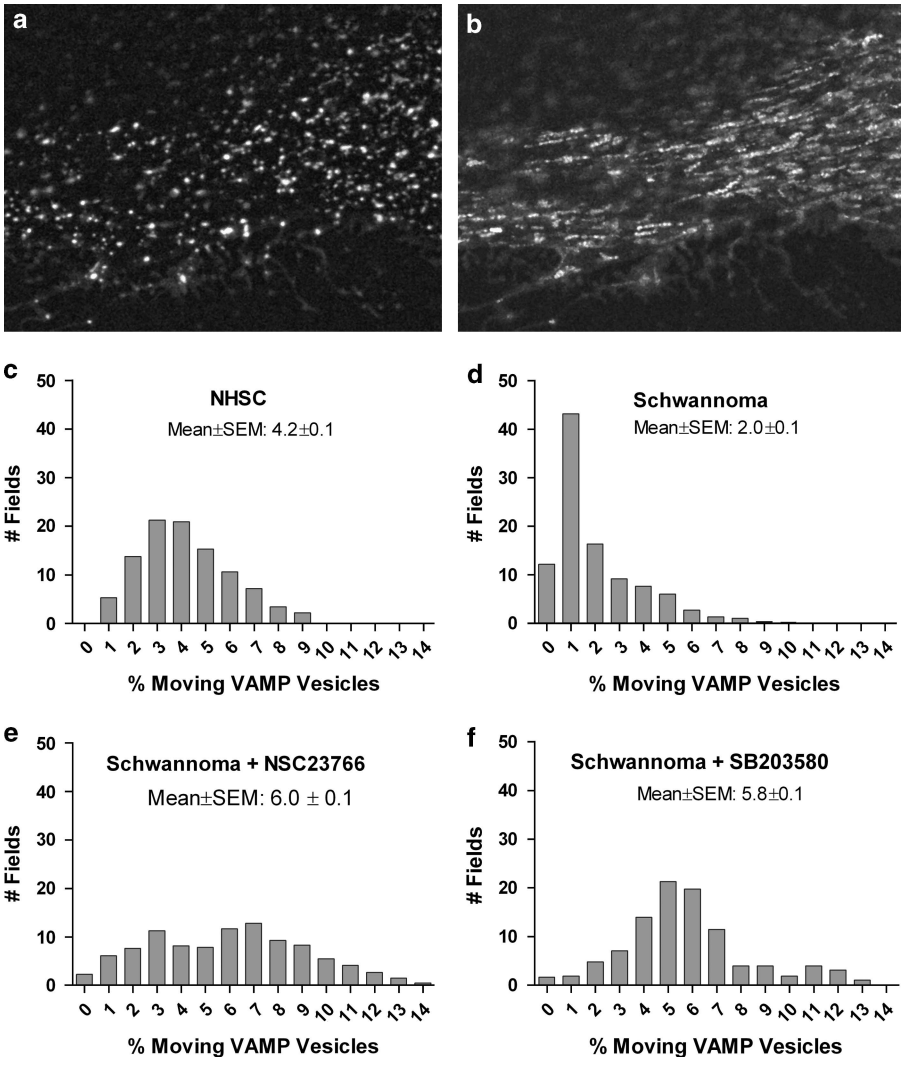

Figure 1. Inhibition of Rac and p38 increases VAMP2-positive vesicle mobility in merlin-null schwannoma. Human schwannoma cells transfected with VAMP-2-GFP-expressing plasmid display a large number of discrete intracellular vesicles (**a**). The cumulative vesicle motility is depicted by combining all images of the time lapse from live cells that were imaged at 3 s intervals for a total of 3 min (**b**). Frequency histograms show the mobile fraction of VAMP2-GFP vesicles per 3 s interval. (**c**) NHSC, mean ± s.e.m.: 4.2 ± 0.1. (**d**) Schwannoma, mean ± s.e.m.: 2.0 ± 0.1. (**e**) Schwannoma + NSC23766, mean ± s.e.m.: 6.0 ± 0.1. (**f**) Schwannoma + SB203580, mean ± s.e.m.: 5.8 ± 0.1.

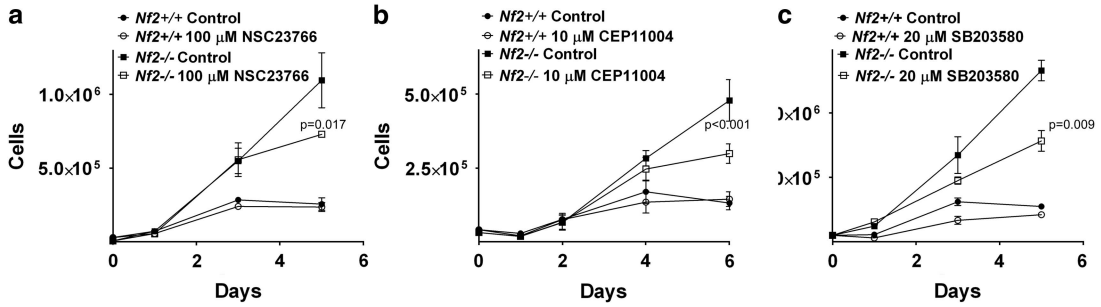

Figure 2. Rac activity specifically regulates high density growth in NF2 null fibroblasts. Immortalized *Nf2+/+* and *Nf2−/−* fibroblasts were plated at low density and allowed to grow to saturation density for 5–6 days in the presence or absence of inhibitors to (**a**) Rac, 100 μM NSC23766 (**b**) MLK, 10 μM CEP11004 and (**c**) $p38^{SAPK}$, 10 μM SB203580.

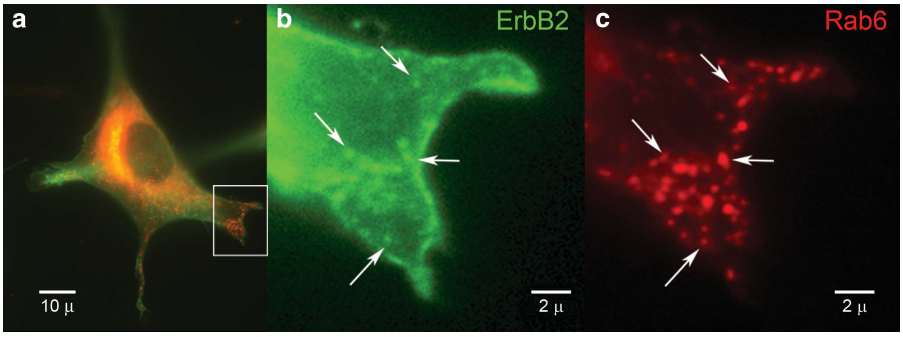

Figure 3. Rab6 vesicles carry ErbB2 cargo. (**a**) Live SC4 cells cotransfected with ErbB2-GFP (green) and Rab6-mStrawberry (red) -expressing plasmids. The box identifies the region shown at high magnification for ErbB2-GFP (**b**) and Rab6-mStrawberry (**c**). The arrows indicate a subset of Rab6-positive intracellular vesicles that contain ErbB2-GFP.

fibroblasts grow to much higher densities than *Nf2+/+* cells, demonstrating merlin-dependent contact inhibition of growth (Figure 2). Treatment with the Rac inhibitor, NSC23766, did not alter growth rates at low density but did significantly inhibit growth of *Nf2−/−* cells once they achieved high density (Figure 2a). Growth rates of *Nf2+/+* cells were unaffected by NSC23766 (Figure 2a). Similarly, CEP11004, an inhibitor of the mixed lineage kinases family (MLK), a Rac effector kinase that regulates $p38^{SAPK}$ activity[28] also specifically inhibited growth once *Nf2−/−* cells achieve high density, but did not affect *Nf2+/+* cells (Figure 2b). The $p38^{SAPK}$ inhibitor, SB203580, slowed growth in *Nf2−/−* at high density but also suppressed the growth rate in *Nf2+/+* cells (Figure 2c). These data suggest that the same signal transduction pathways that affect trafficking are involved in merlin-dependent contact inhibition of growth.

Rab6 is a marker for exocytic vesicles in merlin-deficient schwann cells

The VAMP2-GFP experiments suggested that merlin may regulate intracellular trafficking via Rac in a $p38^{SAPK}$-dependent manner, possibly implicating constitutive exocytosis.[29] We therefore developed a system to specifically measure constitutive exocytosis in an immortalized, transformed merlin-null Schwann cell line, SC4. We used plasmids expressing Rab6 fused to the red fluorescent protein variant mStrawberry as a marker for constitutive exocytosis.[30] To confirm that Rab6 exocytic vesicles carry a cargo relevant to Schwann cells, we cotransfected SC4 cells with plasmids expressing Rab6-mStrawberry and a ErbB2-GFP construct.[31] Images were acquired from live SC4 cells maintained at 37 °C 6 h after transfection, before the bulk of the newly synthesized ErbB2-GFP establishes itself in the plasma membrane. Under these conditions Rab6 was localized primarily to the Golgi with a minority expressed in multiple small vesicles dispersed throughout the cytoplasm (Figure 3a). ErbB2 had plasma membrane localization and a significant amount of nascent ErbB2-GFP in the Golgi but was also localized to small vesicles dispersed within the cytoplasm (Figures 3a and b). A subpopulation of ErbB2-expressing vesicles colocalized with Rab6 vesicles (Figures 3b and c). Time-lapse images of live cells also identified double positive vesicles moving towards the plasma membrane (Supplementary Movie 1). This indicates that a subset of Rab6 positive, post-Golgi vesicles carry the relevant ErbB2 cargo, and confirm Rab6 as a marker of constitutive exocytosis in this system.

Regulation of Rab6 vesicle velocity by the Merlin-Rac-MLK3-$p38^{SAPK}$ pathway

To measure the motion of exocytic Rab6 vesicles, we performed live-cell time-lapse experiments in SC4 cells, maintained at 37 °C (Supplementary Movie 2). A single frame of a representative time lapse shows intense signal in the Golgi with numerous small vesicles dispersed within the cytoplasm (Figure 4a). To visualize motion, all images of the time lapse (60 s) were collated into a single image. This procedure revealed a network of vesicle tracks extending from the Golgi to the plasma membrane, a pattern consistent with vesicles moving along the microtubule network (Figure 4b). To aid in tracking specific vesicles and establish their anterograde direction, time-lapse stacks were color coded to display three successive frames in red, green and blue, then the velocity of individual vesicles was measured (Figure 4c, Supplementary Movie 2).

To test whether merlin loss affects Rab6 vesicle velocity, *Nf2−/−* SC4 cells were cotransfected with plasmids expressing Rab6-mStrawberry and either merlin or empty vector, then velocities were measured as described above. The average

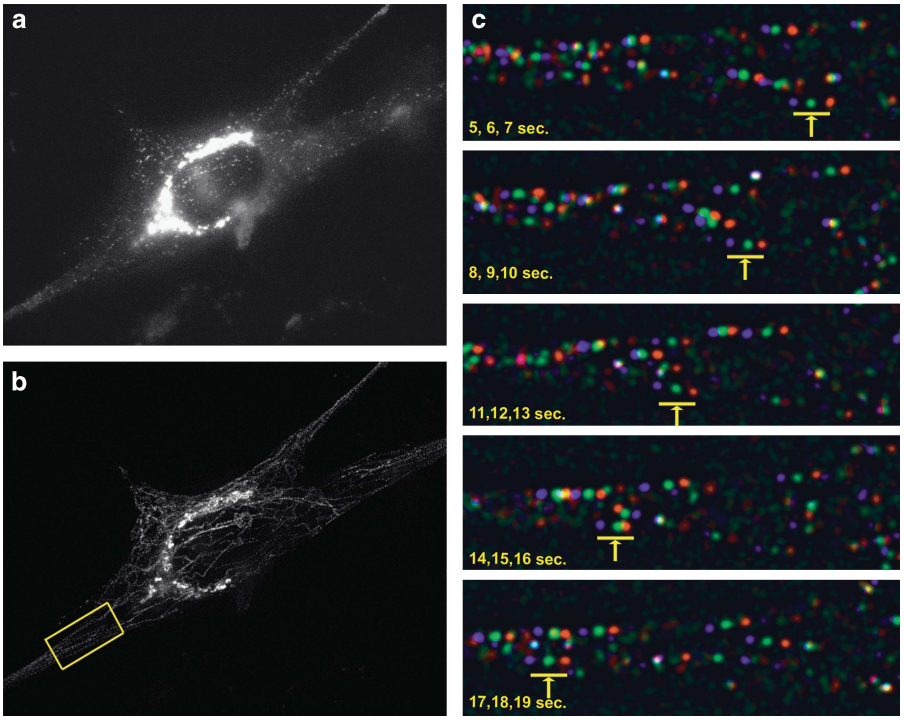

Figure 4. Rab6 exocytic vesicle velocity measurement in live SC4 cells. (**a**) A single frame from a time-lapse SC4 cells transfected with plasmid expressing Rab6-mStrawberry, imaged at 1 s intervals for 1 min. (**b**) Total mobile vesicles depicted by subtracting the minimum pixel projection from the maximum pixel projection. (**c**) Five frames of the time lapse from the region of interest in **b**, processed to facilitate tracking individual vesicles, are shown with successive frames in red, green and blue. The arrow and bar indicates the progress of an individual vesicle over a 10-s time frame.

velocities of 200–500 vesicle tracks per condition were calculated. Re-expression of merlin caused a reproducible shift to a faster moving population of Rab6 vesicles compared to empty vector (Figure 5a). Inhibition of Rac using 100 μM NSC23766 increased vesicle velocity to a similar degree that merlin transfection did (Figure 5b). This suggests that merlin expression in live cells suppresses Rac activity, thereby controlling Rab6 vesicle velocity. Conversely, transfection with a hyperactive fast cycling Rac mutant, F28L, caused a significant decrease in Rab6 vesicle velocity (Figure 5c), consistent with Rac activity acting as a brake on exocytic transport. Interestingly, a constitutively GTP bound, active Rac mutant, Q61L, did not affect Rab6 velocity (Figure 5d), suggesting that the ability of Rac to cycle from the GDP to the GTP-bound states is critical to this regulation. Interestingly, we found that Rac-GTP colocalized with microtubules in SC4 cells (Supplementary Figure 1), consistent with previous reports that Rac-GTP binds to tubulin polymers.[32] These data place active Rac in a position to influence exocytic vesicle transport.

Next, we examined the role of MLK and $p38^{SAPK}$ on exocytic vesicle mobility. Treatment of SC4 cells with the MLK inhibitor CEP11004 increased Rab6 vesicle velocity (Figure 5e), indicating that a member of the MLK family participates in this regulatory pathway. Inhibition of $p38^{SAPK}$ with 20 μM SB203580 also increased Rab6 vesicle velocity (Figure 5f). Taken together these data provide compelling evidence that merlin regulates constitutive exocytosis via a Rac, MLK, $p38^{SAPK}$-mediated pathway.

Open conformation merlin mutants slow anterograde fast axonal transport

To directly assess the effect of Merlin and Rac on microtubule-dependent vesicle traffic, we used vesicle motility assays in isolated squid axoplasm. This experimental system allows for quantitative analysis of fast axonal transport in both anterograde (conventional kinesin-dependent) and retrograde (cytoplasmic dynein-dependent) in the absence of the plasma membrane.[33] Vesicle motility assays in isolated axoplasm were instrumental in the original discovery of conventional kinesin[34] and novel regulatory pathways for microtubule-based vesicle transport.[35,36]

Perfusion of squid axoplasm with 1 μM purified recombinant wild-type merlin protein had little or no inhibitory effect on the velocity of membrane-bound organelles in the anterograde direction over the 50-min assay period (Figure 6a). We then tested FERM-Helix, a C-terminal deletion mutant of merlin containing amino acids 1–502, that was shown to be FERM accessible relative to wild type by virtue of increased interaction with NHERF.[7] Perfusion with the FERM-Helix mutant significantly reduced anterograde vesicle velocity (Figure 6b). Inhibition of $p38^{SAPK}$ activity by coperfusion with the SB203580 inhibitor rescued anterograde vesicle inhibition by the FERM-Helix mutant (Figure 6c). Perfusing a non-phosphorylatable mutant, S518A, had little or no effect on vesicle velocity in this system (Figure 6d), a similar response to wild type. A phosphomimetic mutant S518D, which is predicted to have an accessible FERM domain and fails to suppress cell growth,[13] also reduced anterograde vesicle transport (Figure 6e). This effect was not rescued by SB203580, suggesting different mechanisms of inhibition between FERM-Helix and S518D (Figure 6f). Retrograde velocity was essentially unchanged in all proteins tested. These data suggest that the open, FERM-accessible isoforms of merlin, FERM-Helix and S518D can specifically regulate kinesin-mediated anterograde vesicle transport. This inhibition occurs in the cell-free squid axoplasm system and is thus independent of the plasma membrane, where the bulk of merlin is localized, and of the cell nucleus, another reported site of merlin action.[37] The dependence of FERM-Helix inhibition of anterograde vesicle transport on $p38^{SAPK}$ activity indicates that suppression is mediated by a kinase chain initiated by merlin, leading to a reduction in anterograde vesicle velocity.

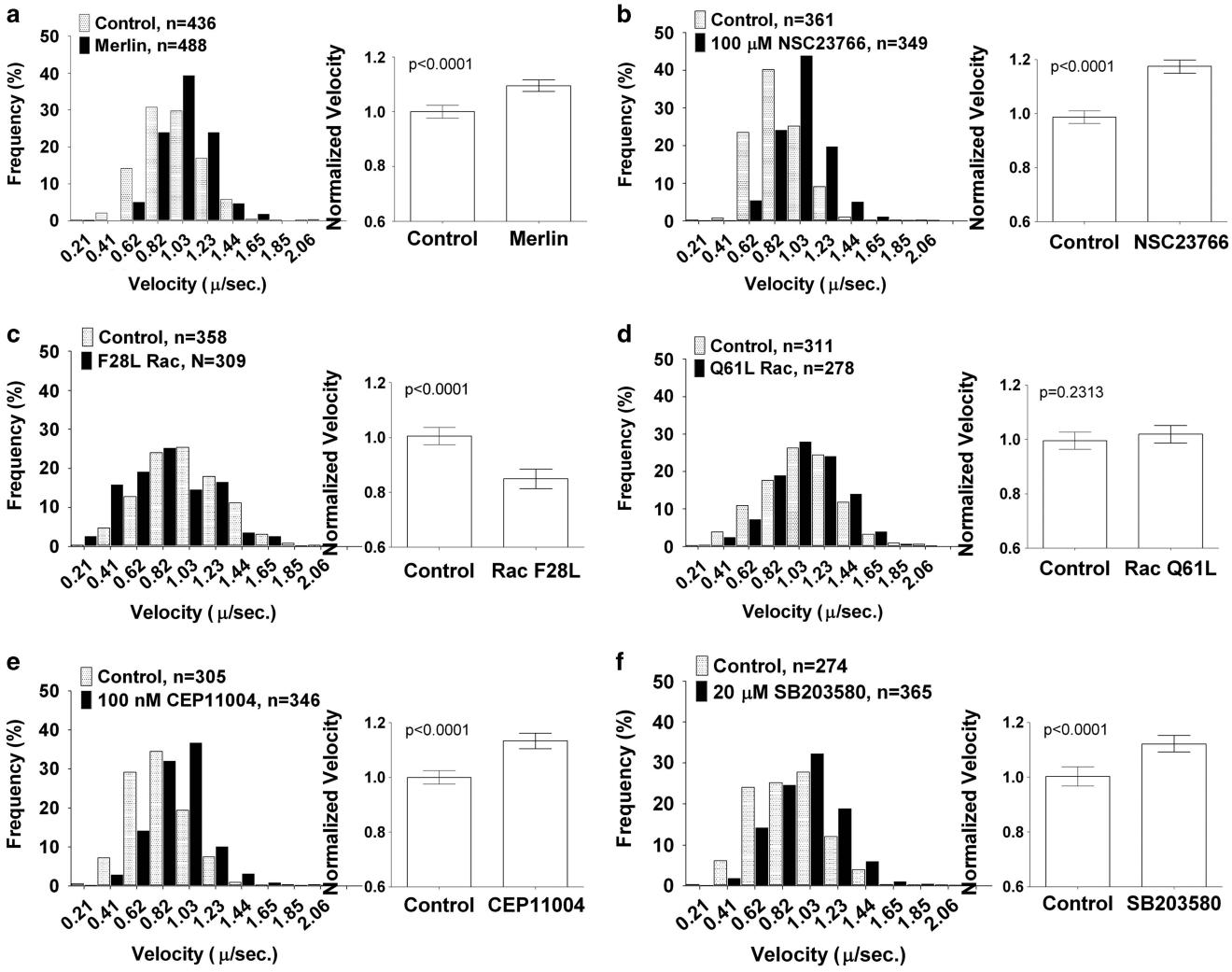

Figure 5. Rab6 vesicle velocity is regulated by a Merlin-Rac pathway. The velocities of anterograde Rab6-mStrawberry exocytic vesicles in transfected SC4 cells displayed as both frequency histograms (left) and a bar graph of mean velocities with the 95% confidence interval (right). (**a**) SC4 cells cotransfected with Rab6-mStrawberry and either a merlin-expressing plasmid or empty vector. (**b**) SC4 cells treated for 2–3 h with 100 μM of the Rac inhibitor NSC23766. (**c**) SC4 cells cotransfected with Rab6-mStrawberry and either an active, fast cycling F28L-Rac mutant-expressing plasmid or empty vector. (**d**) SC4 cells cotransfected with Rab6-mStrawberry and either a constitutively GTP-bound Q61L-Rac mutant-expressing plasmid or empty vector. (**e**) SC4 cells treated for 2–3 h with 100 nM of the MLK inhibitor CEP11004. (**f**) SC4 cells treated for 2–3 h with 20 μM of the $p38^{SAPK}$ inhibitor SB203580.

Rac regulates anterograde fast axonal transport via $p38^{SAPK}$

It is striking that the merlin mutants that inhibit anterograde vesicle transport are predicted to have an open, FERM-accessible conformation and a growth-permissive phenotype. The growth-permissive phenotype correlates with the higher levels of active Rac-GTP, seen in schwannoma cells. In contrast, isoforms that do not affect vesicle transport are predicted to have a closed, FERM-blocked conformation, have a growth-suppression phenotype that correlates with low levels of Rac-GTP. We therefore tested the effect of Rac on anterograde vesicle transport. Perfusion of squid axoplasm with 1 μM active Q61LRac caused a significant and specific reduction in anterograde vesicle transport (Figure 7a). Retrograde transport was unaffected. As with the merlin proteins, inhibition of $p38^{SAPK}$ reversed the effect of Q61L Rac (Figure 7b), suggesting that it functions in the same pathway as merlin to regulate anterograde transport. This effect was specific for active Rac as perfusion with dominant negative N17Rac mutant protein failed to affect either anterograde or retrograde transport (Figure 7c). The effect was also specific for Rac, as perfusion with recombinant active V12 Ras did not affect vesicle transport in either direction (Figure 7c). These results suggest that merlin regulates Rac to control a $p38^{SAPK}$-dependent pathway that specifically regulates anterograde trafficking (Figure 8). Collectively, results from our experiments indicate that the loss of merlin increases Rac activity, which, in turn, promotes activation of the MLK/p38 kinase pathway, ultimately resulting in the inhibition of anterograde vesicle motility.

DISCUSSION

At the cellular level, merlin function is critical for contact inhibition of growth,[8,17] as illustrated by the continued proliferation of *Nf2* null fibroblasts at high cell density,[27] yet the specific biochemical functions that merlin performs remain uncertain. Growing evidence suggests that merlin may control some aspect of intracellular vesicle trafficking.[29,38,39] We hypothesized that merlin regulates anterograde vesicle trafficking and designed a set of experiments to test this hypothesis in the context of live mammalian cells as well as in a plasma membrane-free axoplasm system. Our data suggest that in the absence of merlin active

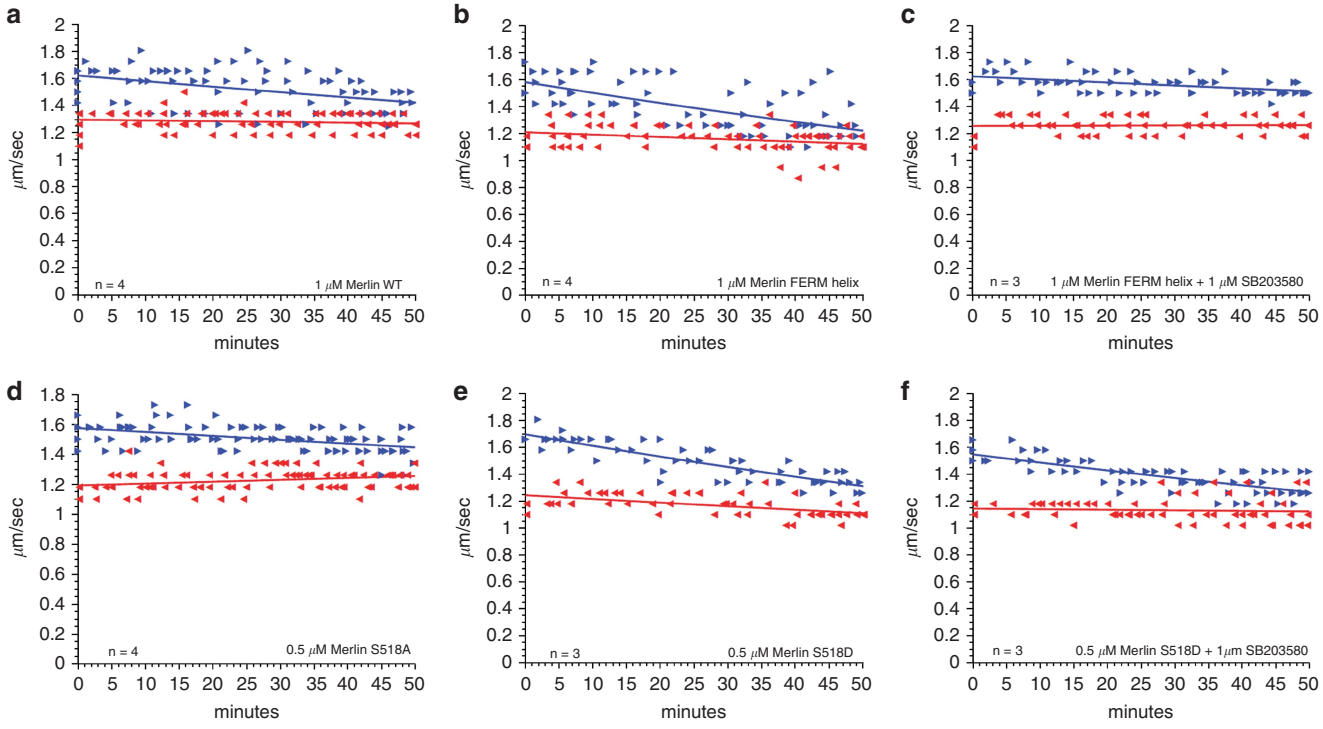

Figure 6. Merlin inhibits anterograde axonal transport in isolated squid axoplasm. Membrane-bound organelle velocities were measured after perfusion of axoplasm with buffer supplemented with 0.5–1 μM purified recombinant merlin, or recombinant merlin plus the $p38^{SAPK}$ inhibitor, SB203580. Anterograde (blue) and retrograde (red) velocity measurements taken between 25 and 45 min were plotted as points. Curves were fitted for anterograde movement and retrograde movement using an exponential curve fit. (**a**) Full length, wild-type merlin. (**b**) C-terminal tail domain deletion mutant, FERM-Helix. (**c**) FERM-Helix plus SB203580. (**d**) The phosphorylation site mutant S518A. (**e**) The phosphomimetic mutant S518D. (**f**) The S518D mutant plus SB203580.

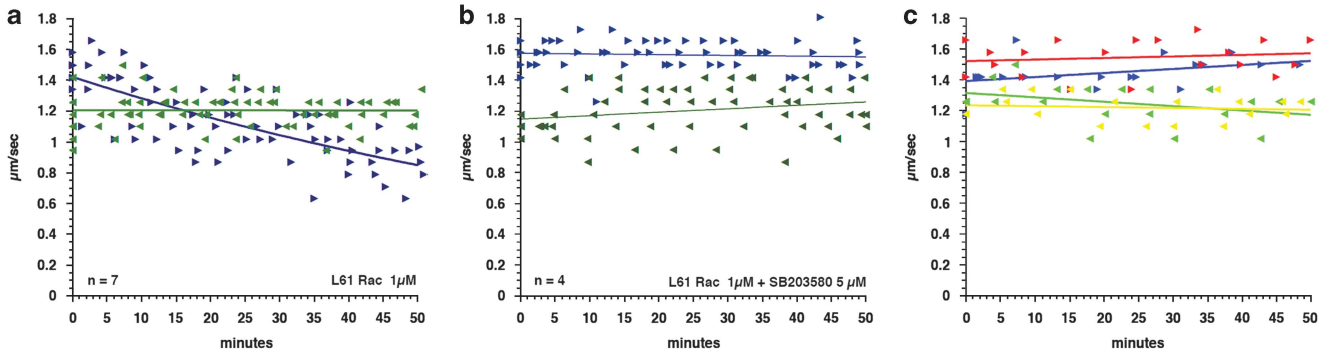

Figure 7. Active Rac inhibits anterograde axonal transport in isolated squid axoplasm. (**a**) 1 μM purified recombinant active Q61L Rac. (**b**) Q61L Rac, treated with the $p38^{SAPK}$ inhibitor, SB203580. (**c**) Dominant negative N17 Rac failed to inhibit anterograde (blue) or retrograde (green). Recombinant active V12 Ha-Ras also failed to inhibit anterograde (red) or retrograde (yellow) transport.

Rac slows kinesin motor-driven transport of vesicles along microtubules. Consistent with this activity, Rac was recently reported to antagonize the function of the mitotic kinesin, Eg5, at microtubule asters during metaphase.[40] This, together with our data, suggests that Rac-mediated signaling pathways may regulate multiple members of the kinesin family.

Our finding that decreased intracellular vesicular trafficking in primary human *NF2* schwannoma cells relative to primary normal human Schwann cells was dependent on Rac, and $p38^{SAPK}$ identifies a novel pathway regulating transport. Notably, the active inhibition of trafficking in merlin-deficient cells by a Rac- and $p38^{SAPK}$-mediated signaling pathway correlated with restored contact inhibition of growth in merlin null fibroblasts, suggesting that this pathway is critical to merlin function. Trafficking experiments in primary human schwannoma cells ensured that the trafficking phenotype is relevant to tumor pathobiology. However, as tumors are the end result of a multi-hit progression, we could not unambiguously attribute changes in vesicle motility to the loss of merlin. Also, because VAMP-2 does not discriminate among different types of intracellular vesicle trafficking,[41] we could not identify the specific molecular systems responsible for changes in vesicle mobility. To address these issues, we designed an experimental system to directly test the effect of merlin on constitutive exocytosis, one of the trafficking modalities implicated in NF2.[29]

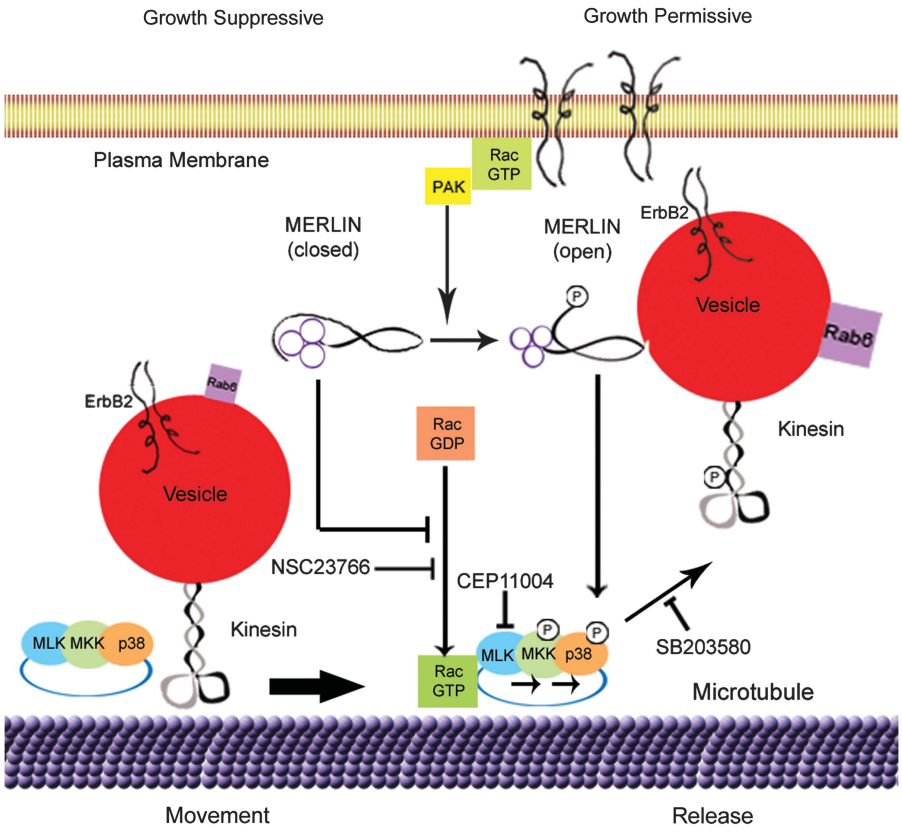

Figure 8. Model for merlin-Rac-p38^{SAPK} regulation of kinesin. A schematic diagram depicting the molecular pathways influenced by merlin and activated Rac that regulate anterograde exocytic vesicle movement by phosphorylation of kinesin heavy chain mediated by the MLK-p38^{SAPK} kinase module.

We used a genetically encoded, fluorescent Rab6-mStrawberry fusion protein to record the trafficking of exocytic vesicles from the Golgi to the plasma membrane.[30] This system focused our analysis on anterograde vesicle movement along microtubules, a direct measure of kinesin motor function in live mammalian cells. Re-expression of merlin or Rac inhibition in *Nf2−/−* SC4 Schwann cells increased Rab6 vesicle velocity. The surprising association of the Rac pathway with vesicle trafficking is strengthened by our finding that inhibition of downstream Rac effectors, MLK and p38^{SAPK}, also significantly increased Rab6 vesicle velocity.

A fast-cycling mutant of Rac, F28L, decreased Rab6 vesicle velocity, providing compelling positive evidence that Rac acts to antagonize anterograde vesicular trafficking. The failure of the constitutive GTP-bound Rac mutant Q61L to reduce vesicle velocity in mammalian cells implies that a specific guanine exchange factor is required, most likely to bind and activate Rac at specific subcellular sites.[42] In contrast, in the squid axoplasm the Rac Q61L did show slow transport. In this case, perfusion of GTP-Rac directly into the axoplasm likely obviated a requirement for nucleotide exchange factors to localize Rac. These results (1) confirm experiments performed in primary schwannoma cells, (2) demonstrate that loss of merlin is sufficient to impair anterograde trafficking and (3) identify a pathway consisting of merlin, Rac, MLK and p38^{SAPK} that modulates microtubule-based trafficking.

The kinesin motor protein heavy chain is a substrate for p38^{SAPK},[26] and kinesin phosphorylation is the most likely mechanism responsible for changes in vesicle kinetics that we describe. A member of the MAP kinase family, p38^{SAPK} is activated by the intermediary kinases, MKK4 and MKK6, which in turn may be activated by MLK.[43,44] MLK itself is activated by binding to Rac-GTP or cdc42-GTP.[45] It is interesting to note that the MLK family member MLK2 can interact with microtubules and complex with the kinesin Kif3,[46] supporting the idea that a Rac-MLK-p38^{SAPK} pathway may have a central role in regulating trafficking of multiple motors.

Use of a plasma membrane-free axoplasm isolated from the giant axon of the Atlantic squid *Loligo pealei* allowed us to distinguish between merlin exerting a direct effect at the level of the microtubules or vesicles and an indirect event caused by merlin regulating upstream signal transduction events originating at the plasma membrane or in the nucleus. Our finding that perfusion of merlin mutants specifically inhibited anterograde transport, argued for a direct regulation of trafficking at the level of microtubules. More significantly this data is consistent with recent reports in the literature, suggesting that merlin interacts with microtubules and promotes tubulin polymerization.[47] In Drosophila, merlin is expressed in cytoplasmic particles that move along microtubules via interaction with kinesin and dynein motor proteins.[48] Inhibition of anterograde trafficking was restricted to the open conformation mutants of merlin, the FERM-Helix domain and S518D. For the FERM-Helix mutant, treatment with the p38^{SAPK} inhibitor SB203580 abrogated this inhibition, confirming that merlin's effect was dependent on a kinase-based signal transduction cascade, most likely targeting the kinesin motor protein complex. The SB203580 did not rescue inhibition by the S518D, suggesting some other mechanism action for this mutant. Regardless of the specific mechanism of action, these intriguing results suggest that presumably growth-permissive forms of merlin may have an active role in orchestrating membrane trafficking during cell growth.

Microtubule-based trafficking is critical for selective delivery of membrane proteins to specific cellular domains in normal cells and tissues. Changes in the regulation of microtubule-based trafficking that alter localization of specific growth factor receptors may be one mechanism by which loss of merlin disrupts contact inhibition of growth. This is consistent with previous observations that merlin regulated growth factor availability,[19,39] endocytosis[38] and exocytosis.[29] Microtubule-based trafficking may have other critical roles in oncogenesis as well. This idea is supported by the fact that activation of kinase-mediated pathways is universal in tumor cells, and recent findings show that many of these same kinases can also affect trafficking. It is therefore of considerable interest to explore this novel relationship between microtubule-based trafficking and cancer.

MATERIALS AND METHODS

Inhibitors

The MLK inhibitor CEP11004 (Cephalon, Frazer, PA, USA) was used at 200 nM final concentration from a 100-μM stock in DMSO. The Rac inhibitor, NSC23766, was a gift from Dr Yi Zheng (Cincinnati Children's Hospital, Cincinnati, OH, USA) used at 100 μM final concentration from a 100-mM aqueous stock. The $p38^{SAPK}$ inhibitor SB203580 (Calbiochem, San Diego, CA, USA) was used at 100 μM final concentration from a 100-mM stock in DMSO.

Plasmids

A plasmid expressing the mStrawberry-Rab6 fusion protein[30] was a kind gift from Dr Anna Akhmanova (Erasmus Medical Center, Rotterdam, The Netherlands). ErbB2 was visualized using pYEC, a gift from Dr Bo van Deus (University of Copenhagen, Copenhagen, Denmark). pYEC expresses a YFP-ErbB2-CFP fusion protein[49] and is referred to in the text as ErbB2-GFP. Rac Q61L (Dr Yi Zheng, Cincinnati Children's Hospital, Cincinnati, OH, USA), Rac-F28L (Dr Yi Zheng, Cincinnati Children's Hospital, Cincinnati, OH, USA), pIRESpuro3 (Clontech, Mountain View, CA, USA), pIRES-Merlin,[7] VAMP2-GFP was a kind gift from Dr Martin ter Beest (University of Chicago, Chicago, IL, USA).

Recombinant proteins

Purified V12HRas-GST, N17Rac-GST and L61Rac-His proteins (Cytoskeleton, Denver, CO, USA) were each reconstituted at 20 μM in ddH_20 and aliquots stored at −80 °C. Recombinant merlin proteins were purified as previously described.[7] Each was perfused into axoplasm in Buffer X/2 with the addition of 5–10 mM Hepes, pH7.2 and 5 mM ATP.

Cell lines

MEF3flox2 and MEF3Δ2 cells were described previously.[27] SC4 *Nf2*−/− Schwann cells were obtained from Dr Helen Morrison (Leibniz Institute for Age Research). Cell lines were maintained in DMEM (Life Technologies, Grand Island, NY, USA) supplemented with 10% fetal bovine serum (Gemini Bioproducts, West Sacramento, CA, USA) and 1% Pen/Strep (HyClone, Logan, UT, USA) at 37 °C, 7.5% CO_2.

Primary cell culture

Primary Schwann cells and schwannoma tumor cells were isolated from normal human nerves and patient-derived schwannomas isolated as previously described.[50,51] For analysis, cells at passage 3–5 were trypsinized and plated onto poly-L-lysine and laminin-coated glass coverslips, and transfected with VAMP-GFP using Fugene-6. After 36–48 h, cells were imaged directly or after 2 h incubation in designated inhibitors.

Growth curves

Nf2+/+ MEF3flox2 and *Nf2*−/− MEF3Δ2 cells each were plated at 50 000 cells per well in replicate six-well plates. Plates were incubated for 6 h, and then were incubated with inhibitor or vehicle in triplicate wells. Plates were incubated overnight then one set was trypsinized and cells were counted with a hemocytometer (Day1). Remaining wells were counted every 48 h until the end of the assay.

Live cell imaging

SC4 cells were plated into 35 mm dishes with a cover slip bottom (Mattek, Ashland, MA, USA), phenol red-free DMEM, 25 mM HEPES pH 7.4, 10% FBS, 1% Pen/Strep supplemented with 20 mM Trolux (Sigma Aldrich, St Louis, MO, USA), as an antifade reagent, then transfected with a mixture of 0.5 μg pRab6-mStrawberry and 1.5 μg either pIRESpuro 3 (Clontech) empty vector or expression vector (merlin, Rac or ErbB2) using Fugene-6 (GE BioSciences, Piscataway, NJ, USA) at a 3:1 Fugene:DNA ratio, as per manufacturer's instructions. Images were acquired on a Zeiss Axiovert 200M microscope equipped with a stage incubator (In Vivo Scientific, St Louis, MO, USA) maintaining 37 °C using an Orca ER II camera (Hammamatsu, Bridgewater, NJ, USA), controlled by MicroManager v1.3 software.[52]

Image analysis

VAMP2 mobility was measured by determining the percentage of VAMP2-GFP-positive pixels that changed position relative to total fluorescence, between each 3 s interval the time lapse. Statistical analysis by Mann–Whitney non-parametric *t*-test and graph generation was performed using Prism (GraphPad, La Jolla, CA, USA).

To image Rab6 vesicle motility, a stack of 60 images were acquired at 1 s intervals with 200 msec exposure with the camera bin set to 2 × 2 for a total of 72 s. Image analysis was performed with Image J software (NIH). To visualize motion, the intensity of small vesicles was enhanced by subtracting a blurred copy of the image, and then all 60 images of the time lapse were collated into a single image. To measure the velocity of individual vesicles, time-lapse stacks were color coded to display successive frames in red, green and blue, the position of individual vesicles was lapse was logged and the distance traveled was measured. At least 21 cells were imaged per replicate with from 10 to 20 tracks measured per cell for a total of 200–500 velocity measurements per experiment. Data was collated and analyzed with Excel (Microsoft). Statistical analysis by Mann–Whitney non-parametric *t*-test and graph generation was performed using Prism (GraphPad).

Axoplasm and video microscopy

Axoplasm was extruded from giant axons dissected from squid (*Loligo pealei*) supplied by the Marine Biological Laboratory (Woods Hole, MA, USA) and video microscopy of membrane-bound organelles and perfusion with recombinant proteins was performed as previously described.[34,53,54]

CONFLICT OF INTEREST

The authors declare no conflict of interest.

ACKNOWLEDGEMENTS

This work was supported by NIH R01 CA118032 (to NR), and MBL research fellowships (to NR and GM), NIH R01 NS23868 (to STB). We thank Atira Dudley Hardiman for assistance with growth and transfection of human cells, Jamie M Walker for expert technical assistance and Dr Yi Zheng for critical reading of the manuscript.

REFERENCES

1 Rouleau GA, Merel P, Lutchman M, Sanson M, Zucman J, Marineau C *et al.* Alteration in a new gene encoding a putative membrane-organizing protein causes neuro-fibromatosis type 2. *Nature* 1993; **363**: 515–521.
2 MacCollin M, Mohney T, Trofatter J, Wertelecki W, Ramesh V, Gusella J. DNA diagnosis of neurofibromatosis 2. Altered coding sequence of the merlin tumor suppressor in an extended pedigree. *JAMA* 1993; **270**: 2316–2320.
3 Ammoun S, Hanemann CO. Emerging therapeutic targets in schwannomas and other merlin-deficient tumors. *Nat Rev Neurol [Review]* 2011; **7**: 392–399.
4 McClatchey AI. Merlin and ERM proteins: unappreciated roles in cancer development? *Nat Rev Cancer* 2003; **3**: 877–883.
5 Giovannini M, Robanus-Maandag E, van der Valk M, Niwa-Kawakita M, Abramowski V, Goutebroze L *et al.* Conditional biallelic Nf2 mutation in the mouse promotes manifestations of human neurofibromatosis type 2. *Genes Dev* 2000; **14**: 1617–1630.
6 Bretscher A, Edwards K, Fehon RG. ERM proteins and merlin: integrators at the cell cortex. *Nat Rev Mol Cell Biol* 2002; **3**: 586–599.
7 Hennigan RF, Foster LA, Chaiken MF, Mani T, Gomes MM, Herr AB *et al.* Fluorescence resonance energy transfer analysis of merlin conformational changes. *Mol Cell Biol* 2010; **30**: 54–67.

8 Shaw RJ, McClatchey AI, Jacks T. Regulation of the neurofibromatosis type 2 tumor suppressor protein, merlin, by adhesion and growth arrest stimuli. *J Biol Chem* 1998; **273**: 7757–7764.
9 Alfthan K, Heiska L, Gronholm M, Renkema GH, Carpen O. Cyclic AMP-dependent protein kinase phosphorylates merlin at serine 518 independently of p21-activated kinase and promotes merlin-ezrin heterodimerization. *J Biol Chem* 2004; **279**: 18559–18566.
10 Jin H, Sperka T, Herrlich P, Morrison H. Tumorigenic transformation by CPI-17 through inhibition of a merlin phosphatase. *Nature* 2006; **442**: 576–579.
11 Xiao GH, Beeser A, Chernoff J, Testa JR. p21-activated kinase links Rac/Cdc42 signaling to merlin. *J Biol Chem* 2002; **277**: 883–886.
12 Kissil JL, Johnson KC, Eckman MS, Jacks T. Merlin phosphorylation by p21-activated kinase 2 and effects of phosphorylation on merlin localization. *J Biol Chem* 2002; **277**: 10394–10399.
13 Shaw RJ, Paez JG, Curto M, Yaktine A, Pruitt WM, Saotome I *et al.* The Nf2 tumor suppressor, merlin, functions in Rac-dependent signaling. *Dev Cell.* 2001; **1**: 63–72.
14 Pelton PD, Sherman LS, Rizvi TA, Marchionni MA, Wood P, Friedman RA *et al.* Ruffling membrane, stress fiber, cell spreading and proliferation abnormalities in human Schwannoma cells. *Oncogene* 1998; **17**: 2195–2209.
15 Kaempchen K, Mielke K, Utermark T, Langmesser S, Hanemann CO. Upregulation of the Rac1/JNK signaling pathway in primary human schwannoma cells. *Hum Mol Genet* 2003; **12**: 1211–1221.
16 Nakai Y, Zheng Y, MacCollin M, Ratner N. Temporal control of Rac in Schwann cell-axon interaction is disrupted in NF2-mutant schwannoma cells. *J Neurosci* 2006; **26**: 3390–3395.
17 Morrison H, Sherman LS, Legg J, Banine F, Isacke C, Haipek CA *et al.* The NF2 tumor suppressor gene product, merlin, mediates contact inhibition of growth through interactions with CD44. *Genes Dev* 2001; **15**: 968–980.
18 Okada T, Lopez-Lago M, Giancotti FG. Merlin/NF-2 mediates contact inhibition of growth by suppressing recruitment of Rac to the plasma membrane. *J Cell Biol* 2005; **171**: 361–371.
19 Curto M, Cole BK, Lallemand D, Liu CH, McClatchey AI. Contact-dependent inhibition of EGFR signaling by Nf2/Merlin. *J Cell Biol* 2007; **177**: 893–903.
20 McClatchey AI, Fehon RG. Merlin and the ERM proteins--regulators of receptor distribution and signaling at the cell cortex. *Trends Cell Biol* 2009; **19**: 198–206.
21 Sampo B, Kaech S, Kunz S, Banker G. Two distinct mechanisms target membrane proteins to the axonal surface. *Neuron* 2003; **37**: 611–624.
22 Gerst JE. SNAREs and SNARE regulators in membrane fusion and exocytosis. *Cell Mol Life Sci* 1999; **55**: 707–734.
23 Singh BB, Lockwich TP, Bandyopadhyay BC, Liu X, Bollimuntha S, Brazer SC *et al.* VAMP2-dependent exocytosis regulates plasma membrane insertion of TRPC3 channels and contributes to agonist-stimulated Ca2 + influx. *Mol Cell* 2004; **15**: 635–646.
24 Randhawa VK, Bilan PJ, Khayat ZA, Daneman N, Liu Z, Ramlal T *et al.* VAMP2, but not VAMP3/cellubrevin, mediates insulin-dependent incorporation of GLUT4 into the plasma membrane of L6 myoblasts. *Mol Biol Cell* 2000; **11**: 2403–2417.
25 Gao Y, Dickerson JB, Guo F, Zheng J, Zheng Y. Rational design and characterization of a Rac GTPase-specific small molecule inhibitor. *Proc Natl Acad Sci USA* 2004; **101**: 7618–7623.
26 Bosco DA, Morfini G, Karabacak NM, Song Y, Gros-Louis F, Pasinelli P *et al.* Wild-type and mutant SOD1 share an aberrant conformation and a common pathogenic pathway in ALS. *Nat Neurosci* 2010; **13**: 1396–1403.
27 Bosco EE, Nakai Y, Hennigan RF, Ratner N, Zheng Y. NF2-deficient cells depend on the Rac1-canonical Wnt signaling pathway to promote the loss of contact inhibition of proliferation. *Oncogene* 2010; **29**: 2540–2549.
28 Tibbles LA, Ing YL, Kiefer F, Chan J, Iscove N, Woodgett JR *et al.* MLK-3 activates the SAPK/JNK and p38/RK pathways via SEK1 and MKK3/6. *EMBO J* 1996; **15**: 7026–7035.
29 Lallemand D, Manent J, Couvelard A, Watilliaux A, Siena M, Chareyre F *et al.* Merlin regulates transmembrane receptor accumulation and signaling at the plasma membrane in primary mouse Schwann cells and in human schwannomas. *Oncogene* 2009; **28**: 854–865.
30 Grigoriev I, Splinter D, Keijzer N, Wulf PS, Demmers J, Ohtsuka T *et al.* Rab6 regulates transport and targeting of exocytotic carriers. *Dev Cell* 2007; **13**: 305–314.
31 Lerdrup M, Hommelgaard AM, Grandal M, van Deurs B. Geldanamycin stimulates internalization of ErbB2 in a proteasome-dependent way. *J Cell Sci* 2006; **119**(Part 1): 85–95.
32 Best A, Ahmed S, Kozma R, Lim L. The Ras-related GTPase Rac1 binds tubulin. *J Biol Chem* 1996; **271**: 3756–3762.
33 Morfini GA, Burns M, Binder LI, Kanaan NM, LaPointe N, Bosco DA *et al.* Axonal transport defects in neurodegenerative diseases. *J Neurosci* 2009; **29**: 12776–12786.
34 Brady ST, Lasek RJ, Allen RD. Video microscopy of fast axonal transport in extruded axoplasm: a new model for study of molecular mechanisms. *Cell Motil* 1985; **5**: 81–101.
35 Morfini G, Pigino G, Szebenyi G, You Y, Pollema S, Brady ST. JNK mediates pathogenic effects of polyglutamine-expanded androgen receptor on fast axonal transport. *Nat Neurosci* 2006; **9**: 907–916.
36 Morfini GA, You YM, Pollema SL, Kaminska A, Liu K, Yoshioka K *et al.* Pathogenic huntingtin inhibits fast axonal transport by activating JNK3 and phosphorylating kinesin. *Nat Neurosci* 2009; **12**: 864–871.
37 Li W, You L, Cooper J, Schiavon G, Pepe-Caprio A, Zhou L *et al.* Merlin/NF2 suppresses tumorigenesis by inhibiting the E3 ubiquitin ligase CRL4(DCAF1) in the nucleus. *Cell* 2010; **140**: 477–490.
38 Maitra S, Kulikauskas RM, Gavilan H, Fehon RG. The tumor suppressors merlin and Expanded function cooperatively to modulate receptor endocytosis and signaling. *Curr Biol* 2006; **16**: 702–709.
39 Cole BK, Curto M, Chan AW, McClatchey AI. Localization to the cortical cytoskeleton is necessary for Nf2/merlin-dependent epidermal growth factor receptor silencing. *Mol Cell Biol* 2008; **28**: 1274–1284.
40 Woodcock SA, Rushton HJ, Castaneda-Saucedo E, Myant K, White GR, Blyth K *et al.* Tiam1-Rac signaling counteracts Eg5 during bipolar spindle assembly to facilitate chromosome congression. *Curr Biol* 2010; **20**: 669–675.
41 Chen YA, Scheller RH. SNARE-mediated membrane fusion. *Nat Rev Mol Cell Biol [Review]* 2001; **2**: 98–106.
42 Bos JL, Rehmann H, A Wittinghofer. GEFs and GAPs: critical elements in the control of small G proteins. *Cell* 2007; **129**: 865–877.
43 Avruch J. MAP kinase pathways: The first twenty years. *Bba-Mol Cell Rea* 2007 1150–1160.
44 Gallo KA, Johnson GL. Mixed-lineage kinase control of JNK and p38 MAPK pathways. *Nat Rev Mol Cell Biol. [Review]* 2002; **3**: 663–672.
45 Teramoto H, Coso OA, Miyata H, Igishi T, Miki T, Gutkind JS. Signaling from the small GTP-binding proteins Rac1 and Cdc42 to the c-Jun N-terminal kinase/stress-activated protein kinase pathway. A role for mixed lineage kinase 3/protein-tyrosine kinase 1, a novel member of the mixed lineage kinase family. *J Biol Chem* 1996; **271**: 27225–27228.
46 Nagata K, Puls A, Futter C, Aspenstrom P, Schaefer E, Nakata T *et al.* The MAP kinase kinase kinase MLK2 co-localizes with activated JNK along microtubules and associates with kinesin superfamily motor KIF3. *EMBO J.* 1998; **17**: 149–158.
47 Muranen T, Gronholm M, Lampin A, Lallemand D, Zhao F, Giovannini M *et al.* The tumor suppressor merlin interacts with microtubules and modulates Schwann cell microtubule cytoskeleton. *Hum Mol Genet* 2007; **16**: 1742–1751.
48 Bensenor LB, Barlan K, Rice SE, Fehon RG, Gelfand VI. Microtubule-mediated transport of the tumor-suppressor protein merlin and its mutants. *Proc Natl Acad Sci USA* 2010; **107**: 7311–7316.
49 Lerdrup M, Bruun S, Grandal MV, Roepstorff K, Kristensen MM, Hommelgaard AM *et al.* Endocytic down-regulation of ErbB2 is stimulated by cleavage of its C-terminus. *Mol Biol Cell* 2007; **18**: 3656–3666.
50 Rutkowski JL, Kirk CJ, Lerner MA, Tennekoon GI. Purification and expansion of human Schwann cells in vitro. *Nat Med* 1995; **1**: 80–83.
51 Rosenbaum C, Kluwe L, Mautner VF, Friedrich RE, Muller HW, Hanemann CO. Isolation and characterization of Schwann cells from neurofibromatosis type 2 patients. *Neurobiol Dis* 1998; **5**: 55–64.
52 Edelstein A, Amodaj N, Hoover K, Vale R, Stuurman N. *Computer Control of Microscopes Using μManager*. John Wiley & Sons, Inc, 2010.
53 Brady ST, Pfister KK, Bloom GS. A monoclonal antibody against kinesin inhibits both anterograde and retrograde fast axonal transport in squid axoplasm. *Proc Natl Acad Sci USA* 1990; **87**: 1061–1065.
54 Stenoien DL, Brady ST. Immunochemical analysis of kinesin light chain function. *Mol Biol Cell* 1997; **8**: 675–689.

Supplementary information accompanies the paper on the Oncogene website (http://www.nature.com/onc)